Electronic Supplementary Material (ESI) for RSC Advances.

Supporting Information

A well fabricated PtSn/SiO_2 catalyst with enhanced synergy between Pt and Sn for acetic acid hydrogenation into ethanol

Guozhen Xu, Jian Zhang*, Shengping Wang, Yujun Zhao*, and Xinbin Ma

Key Laboratory for Green Chemical Technology of Ministry of Education, Collaborative Innovation Centre of Chemical Science and Engineering, School of Chemical Engineering and Technology, Tianjin University, Tianjin 300072, China

* Corresponding author:

Dr. Jian Zhang, Tel. & fax: 022-87401818, E-mail: zhangjian1985@tju.edu.cn

Prof. Yujun Zhao, Tel. & fax: 022-87401818, E-mail: yujunzhao@tju.edu.cn

Table of Contents

1. BET results of the reduced catalysts

2. EDX elemental-mapping analysis of the PtSn1.6/SiO_2-MTSG catalyst

3. TPR measurements

4. TEM images of the reduced PtSnx/SiO_2-MTSG catalysts

5. Integral results of Lewis acid sites

6. The influence of kinetics parameters on the catalytic performance

1. BET results of the reduced catalysts

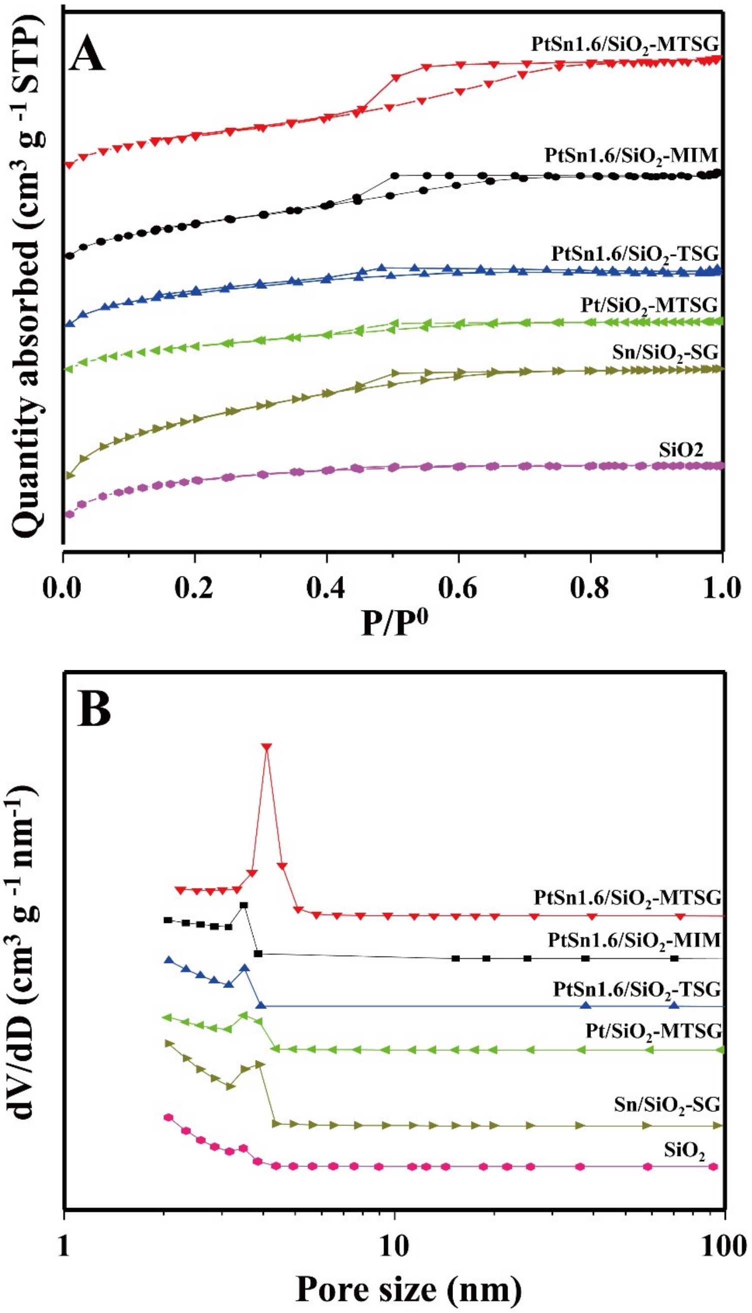

Fig. S1. A) N_2 adsorption-desorption isotherms, B) pore size distribution of reduced catalysts.

The N_2 adsorption-desorption isotherms of the reduced catalysts are exhibited in Fig. S1A. All the samples display type IV hysteresis loop isotherms, indicating that the mesoporous structures are largely maintained after the incorporation of Pt and Sn precursors. Pore size distribution obtained from the desorption branches of the N_2

isotherms using the BJH method reveals that SiO_2 and Sn/SiO_2-SG support have narrow pore size distribution as illustrated in Fig. S1B. The BET surface area for the Sn/SiO_2-SG support is 975 $m^2 \cdot g^{-1}$, which is much higher than the PtSn/SiO_2 catalysts (400-600$m^2 \cdot g^{-1}$) (listed in Table 1). The decrease in the specific surface area may be caused by the blocking of partial pore structure when Pt is uploaded. Additionally, the Sn/SiO_2-SG support exhibit an appropriate pore size and pore distribution, which facilitate the dispersion of metal particles. As to the PtSn/SiO_2 catalysts, the PtSn1.6/SiO_2-MTSG catalyst displays a slight superiority in the specific pore size and distribution.

2. EDX elemental-mapping analysis of the PtSn1.6/SiO$_2$-MTSG catalyst

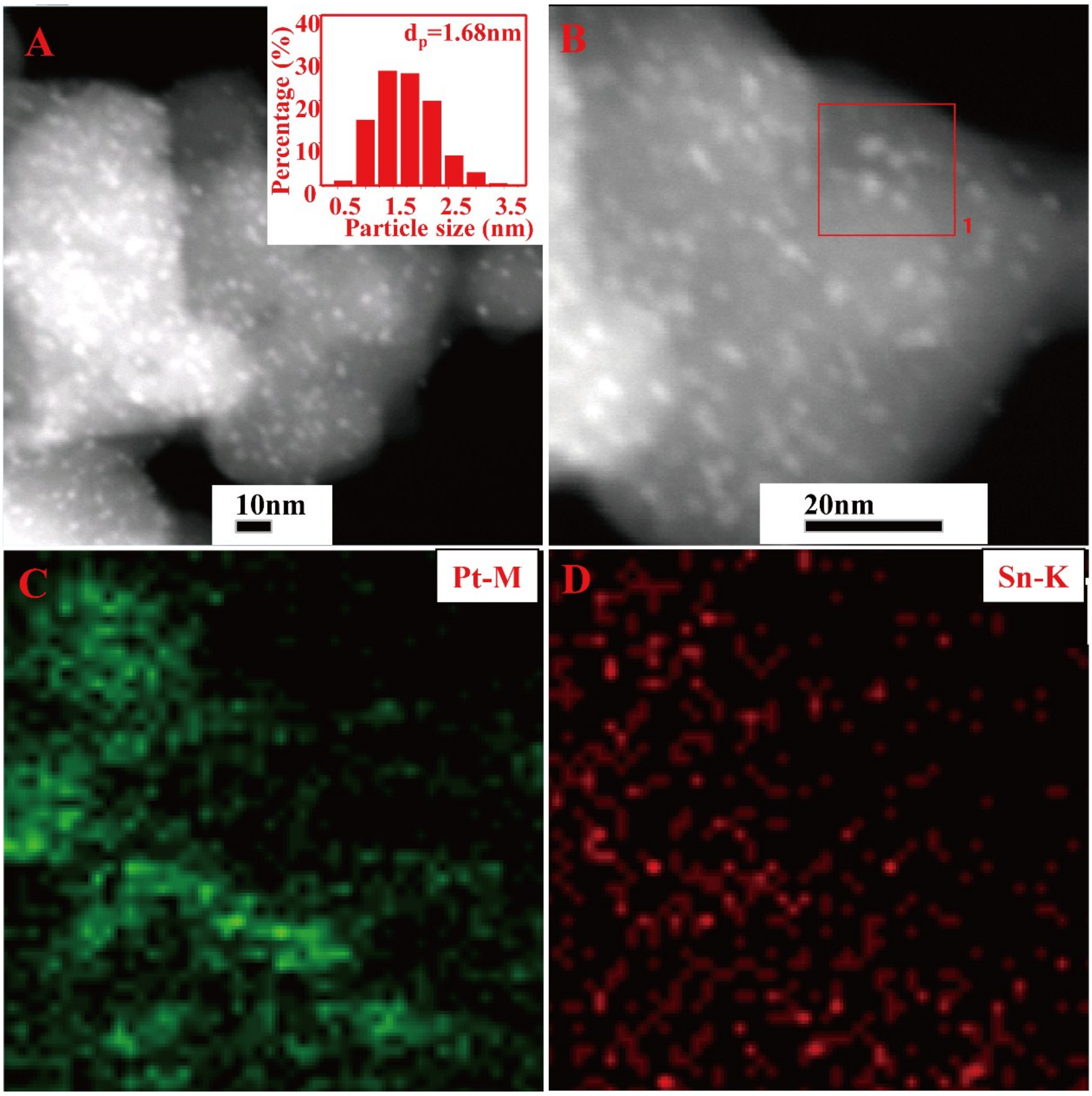

Fig. S2. A, B) HAADF-STEM images. C, D) EDX elemental-mapping images of the reduced PtSn1.6/SiO$_2$-MTSG catalyst.

3. TPR measurements

Table S1. Fitted results of H_2-TPR experiments of catalysts

Catalyst	T_M			Total consumption (mmol/g)	Consumption (mmol/g)		
	I	II	III		I	II	III
Sn/SiO_2-SG	--	--	503	0.062	--	--	0.062
Pt/SiO_2-MTSG	206	366	--	0.062	0.022	0.040	--
PtSn1.6/SiO_2-MTSG	--	282	430	0.071	--	0.054	0.017
PtSn1.6/SiO_2-MIM	--	272	360	0.076	--	0.050	0.026
PtSn1.6/SiO_2-TSG	91	193	420	0.066	0.015	0.039	0.012

4. TEM images of the reduced PtSnx/SiO_2-MTSG catalysts

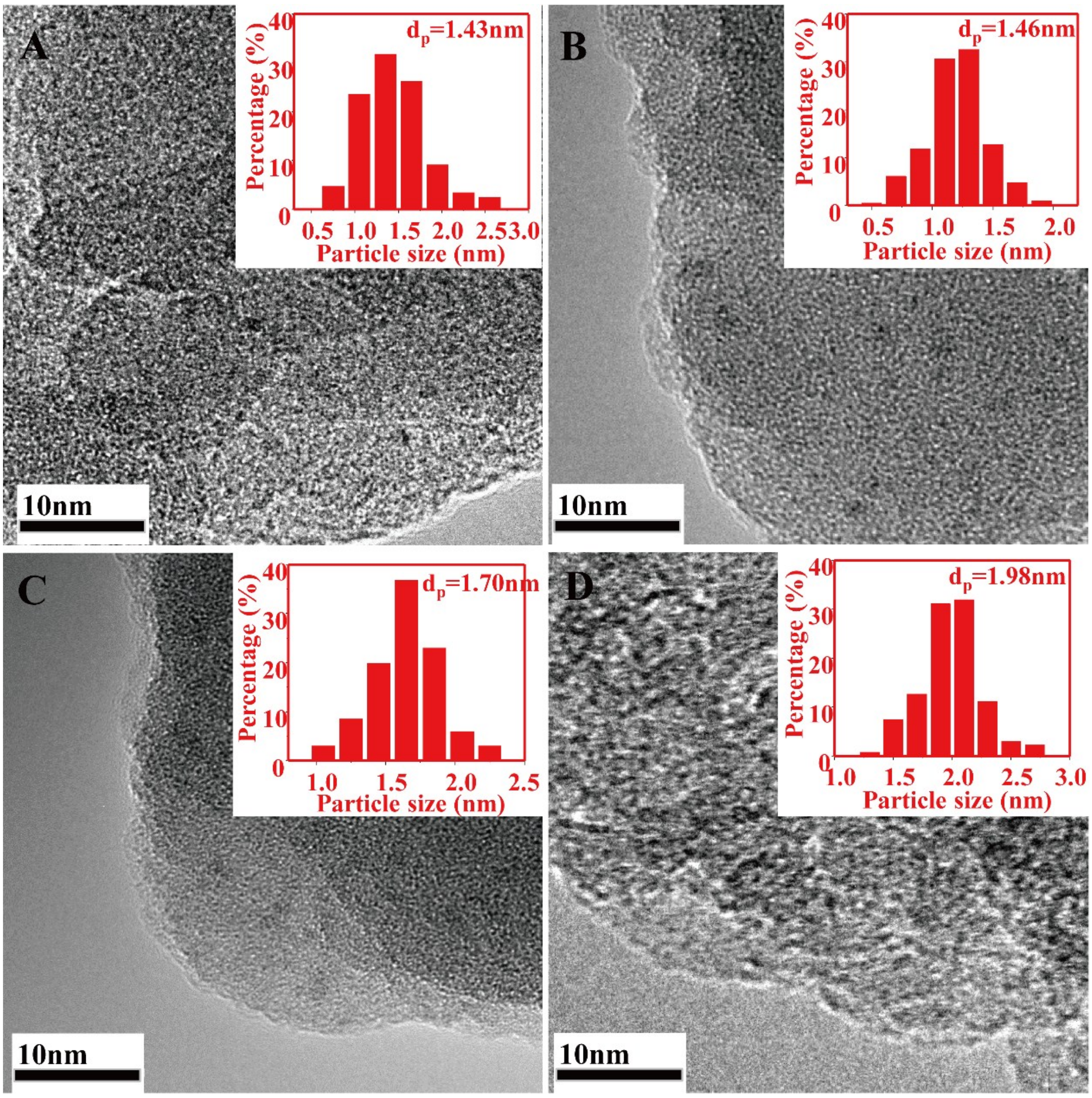

Fig. S3. TEM images of the reduced PtSnx/SiO_2-MTSG catalysts. A) PtSn1.0/SiO_2-MTSG, B) PtSn1.6/SiO_2-MTSG, C) PtSn3.3/SiO_2-MTSG, D) PtSn8.2/SiO_2-MTSG.

5. Integral results of Lewis acid sites

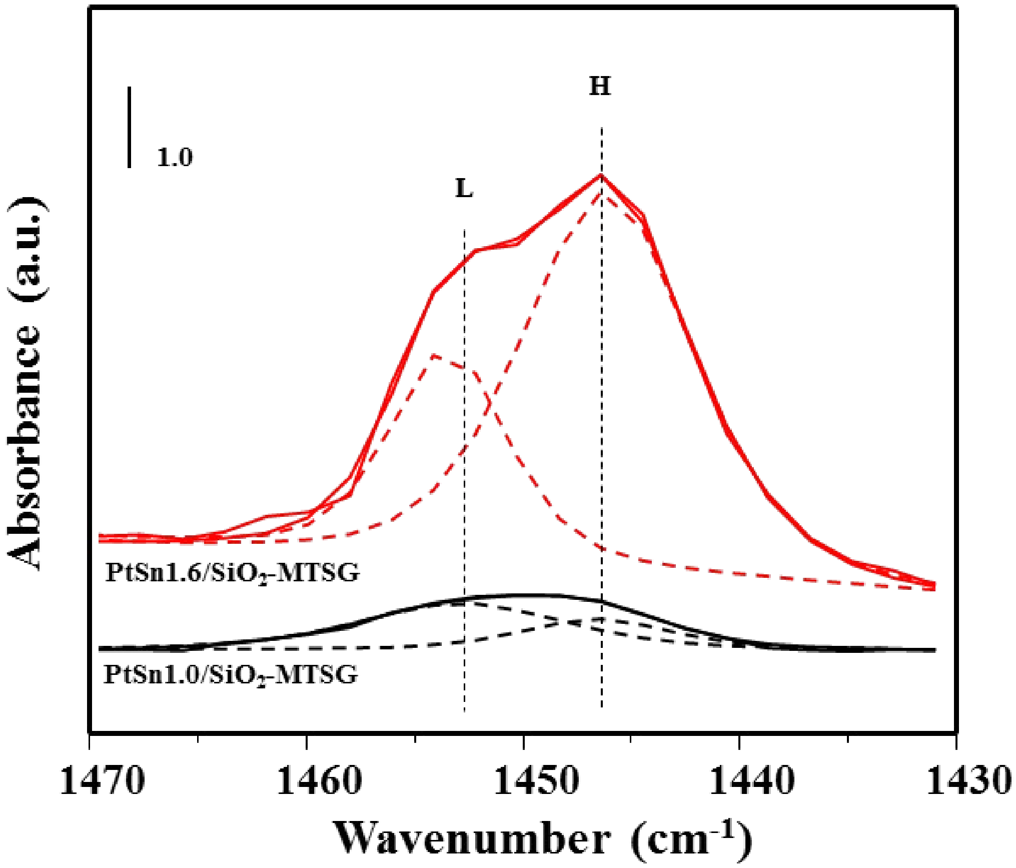

Fig. S4. Deconvolution of the fit about FTIR spectra of chemisorbed pyridine on reduced catalysts.

Table S2. Integral quantity of Lewis acid sites of reduced catalysts [a].

Catalyst	PtSn1.0/SiO$_2$-MTSG	PtSn1.6/SiO$_2$-MTSG	PtSn3.3/SiO$_2$-MTSG	PtSn8.2/SiO$_2$-MTSG
Lewis acid sites (μmol·g^{-1}) [b]	5.1	13.4	14.4	56.4

[a] Catalysts determined when pyridine was adsorbed at 50 °C and outgassed at 150 °C.

[b] Amount of adsorbed pyridine (integration regions approximately at 1430-1470cm^{-1}).

6. The influence of kinetics parameters on the catalytic performance

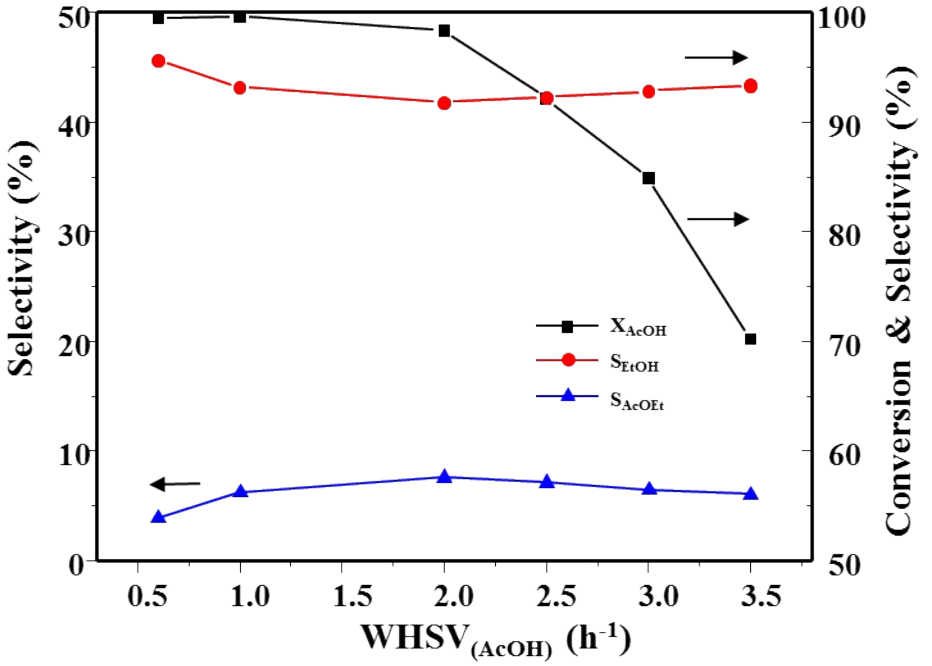

Fig. S5. Hydrogenation performance of AcOH over PtSn1.6/SiO_2-MTSG catalyst as a function of WHSV$_{(AcOH)}$. Reaction conditions: 270 °C, 2.6 MPa, H_2/AcOH (mol/mol) = 20.

Table S3. Hydrogenation performance of AcOH over PtSn1.6/SiO_2-MTSG catalysts

WHSV (h^{-1})	Conv. (%)	Selectivity (%)	
		EtOH	AcOEt
1[a]	99.7	91.0	8.1
2[a]	98.9	86.6	12.4
3[a]	86.9	87.2	12.0
1[b]	97.8	91.7	8.0
2[b]	71.0	93.1	6.5
3[b]	51.8	93.9	5.7
1[c]	96.4	91.2	7.8
2[c]	67.3	92.5	6.4
3[c]	49.5	93.0	5.9

[a] Reaction conditions: 270 °C, 2.6 MPa, H_2/AcOH (mol/mol) = 10.

[b] Reaction conditions: 250 °C, 2.6 MPa, H_2/AcOH (mol/mol) = 20.

[c] Reaction conditions: 270 °C, 1.5 MPa, H_2/AcOH (mol/mol) = 20.

As listed in Table S3, the influence of space velocity of AcOH ($WHSV_{(AcOH)}$) on the catalytic performance were evaluated at different reaction conditions. Conversion of AcOH decreases with the increase of $WHSV_{(AcOH)}$ at all different reaction conditions. Ethanol selectivity firstly decreases with the increase of $WHSV_{(AcOH)}$ and then remains unchanged when $WHSV_{(AcOH)}$ is further increased at the conditions: 270°C, 2.6 MPa, H_2/AcOH (molar ratio) = 10. When the reaction was conducted at 250 °C, selectivity of ethanol remains the same with the increase of $WHSV_{(AcOH)}$. Similarly, ethanol selectivity hardly changes with the increase of $WHSV_{(AcOH)}$ at the pressure of 1.5 MPa.